Hindawi
Journal of Engineering
Volume 2022, Article ID 3552675, 10 pages
https://doi.org/10.1155/2022/3552675

Research Article

Effect of SiC Addition on Microhardness and Relative Density during Selective Laser Melting of 316L Stainless Steel

Raid Mohammed Hadi and Ziad Aeyad Taha

Institute of Laser for Postgraduate Studies, University of Baghdad, Baghdad, Iraq

Correspondence should be addressed to Raid Mohammed Hadi; raed.mohammed1001a@ilps.uobaghdad.edu.iq

Received 1 July 2022; Revised 5 October 2022; Accepted 14 October 2022; Published 15 November 2022

Academic Editor: Konstantinos Salonitis

The utilization of 316L stainless steel has been very common in marine, automotive, architectural, and biomedical applications due to its adequate corrosion resistance to cracks after the completion of welding process. However, there has been ongoing attempts to investigate the potential enhancement in the strength and durability of 316L stainless steel by reinforcing it with silicon carbide (SiC). The present work adopts the selective laser melting (SLM) technique to fabricate SiC-reinforced 316L steel to boost its microhardness and strength properties. The methodology involved the addition of 1% wt. silicon carbide with particle sizes <40 μm to reinforce the stainless steel matrix. An SLM metal printing machine equipped with a continuous wave of 300 W fiber laser is employed to form the specimens. To measure the properties of the final product, EDX, XRD, FESEM, and universal tensile test machines have been used. The maximum value of 296 HV was obtained for a 1% volume of SiC compared to the 285 HV microhardness of pure stainless steel 316L. FESEM examination showed that the SiC microparticles were dissolved completely and they were randomly distributed in the melting basin. The samples were dissolved entirely, and the best porosity was obtained at 0.4% with influential parameters of 200 W laser power, 70 μm hatching distance, 30 μm layer thickness, and 700 mm/s velocities. The results also revealed that the microhardness at these parameters is the best compared to the samples produced with different values. The volumetric energy density was also considered. The findings can be informative to the researchers and manufacturers interested in 316L steel industry.

1. Introduction

Lasers are utilized in a variety of industries including welding, drilling, cleaning, ablation, and so on [1–5]. Additive manufacturing is an emerging field for lasers in industrial applications, and it has a promising future. The additive manufacturing (AM) technique is defined by ASTM International as the process of joining materials to build parts or objects from 3D model data, usually layer upon layer, in contrast to subtractive manufacturing methodologies [6]. Metal matrix composites (MMCs) are typically fabricated by continuous spreading for a reinforcing into a monolithic metallic material matrix [7]. A metallic matrix is typically combined with strong ceramic reinforcements to create metal matrix composites (MMCs). Traditional examples of hard ceramic materials that are used as reinforcements are SiC, TiC, B_4C, Al_2O_3, TiB_2, and ZrO_2. The main reason for using silicon carbide (SiC) as a reinforcement material is because of certain distinct advantages that are usually non-existent in other reinforcements, such as low cost, adequate hardness, and excellent corrosion resistance in addition to its resistance to oxidation at high temperatures [8, 9]. Additive manufacturing (AM) (also called 3D printing technique) allows for the construction of very complex geometries in metals, ceramics, composites, and polymers that are impossible to be fabricated using traditional subtractive processing methods [10–12]. The laser powder bed fusion (LPBF) is an effective laser-based AM technology that has been lately employed for fabricating complex metal components. This technology is also known as selective laser melting (SLM) [13, 14]. The SLM has sparked broad interest due to its advantages concerning design flexibility and efficient production, which overcome the limits of traditional processing technologies [15, 16]. In the SLM process, a beam scans over a powder bed and selectively melts powder particles to form 3D objects layer by layer according to the layout in a computer-aided design file [17–21]. The process of SLM has been found appropriate for several materials, especially for the metal alloys used in engineering [22–25]. It is agreed that the SLM technology has significant popularity as a speedy prototyping technique with a delicate microstructure because of the high cooling rate which could lead to yielding a solidification process that is non-equilibrium. As a consequence, the process can produce special characteristics regarding aspects such as microstructures, chemical composition, phase, and mechanical properties [26]. Nevertheless, one of the recognized disadvantages of this process is the limitation of the sample size, which is related to the issue of elaborating the dimensions of chamber [27, 28]. According to the literature, in aerospace, marine, and biomedical applications, the widely used alloy is the austenitic stainless steel, mainly due to two of its outstanding properties—corrosion resistance and ductility [29]. Furthermore, it was reported that the specific recognized austenitic stainless steel's properties, such as adequate formability and excellent resistance to oxidation and corrosion, have popularized its use in several modern industries as an engineering material [30].

Asif Ur Rehman et al. investigated the influence of SiC particles on Al_2O_3 in powder bed selective laser process (PBSLP). It was reported that the use of silicon carbide as an additive can aid in averting the appearance of cracks; this is usually accomplished by two mechanisms: crack deflection and crack pinning. During both the classical and additive manufacturing techniques, Al_2O_3 and SiC have several applications when Al_2O_3 is adopted as a matrix or when it is used as an additive in the silicon carbide [31]. When SiC is used to boost 316L metallic matrix composites, it influenced the densification effectiveness, microstructure development, crystallographic orientation, and tribology-related properties [32]. The potential influence of the processing factors of direct laser deposition (DLD) additive manufacturing of 316L/SiC metal matrix composites on the microhardness and structure of the resulting samples was examined [33]. Due to the combined properties of the Al matrix and reinforcements such as SiC/Al, it was demonstrated that particulate-reinforced aluminum matrix composites (PAMCs) are significant materials for many applications [34]. The density, microhardness, and parts produced with varied particle sizes and mass fractions of TiC with 316L stainless steel were also studied [35]. The effects of the Gr content on dry sliding wear and hardness were explored, and according to the findings, a composite with good tribological performance can be efficiently manufactured via SLM [36].

This study aims to manufacture a product from AISI 316L that is reinforced with only 1% silicon carbide to improve the mechanical properties using the selective laser melting technique. The current study used laser parameters and particle sizes for steel and silicon carbide that mostly differ from those adopted in the studies previously mentioned.

2. Materials and Methods

The experimental process involved the use of commercial 316L stainless steel powder obtained by gas atomization with particle sizes <65 μm. Figure 1 illustrates that the SS 316L powder is spherical after being examined by a scanning electron microscope (SEM). Figure 2 demonstrates the energy-dispersive X-ray spectrometry (EDX) for stainless steel sample products where the proportions of elements in stainless steel can be observed.

The silicon carbide with particle sizes <40 μm was used as an additive to reinforce the stainless steel matrix. A certain percentage of silicon carbide grade (1% wt) has been added to investigate their potential effects on the microhardness and relative density of stainless steel 316L manufactured by SLM. The composite powder was created utilizing mechanical mixing in a ball mill with a rotation speed of 100 rpm for 45 minutes. The average chemical composition of the stainless steel is illustrated in Table 1. Cubic specimens with dimensions of $(10\times10\times10)$ mm^3, as depicted in Figure 3, have been fabricated from stainless steel 316L with 1% silicon carbide.

An SLM metal printing machine (M100) of laboratory scale that is equipped with a continuous wave of 300 W fiber laser and an approximate laser beam of 80 μm was employed to form the specimens. All the considered specimens were of 30 μm thickness and their process was performed under an argon atmosphere. The objective is to as much as possible avoid the oxidation phenomenon that might occur during laser melting. For pure stainless steel substrate, the process was performed under 80°C, and no heat-specialized action was considered to treat the specimens after fabrication. The volumetric energy density can be computed using equation (1). The volumetric energy density (VED) represents the total input energy to the material per unit volume during the SLM process, usually expressed in J/mm^3 [22].

$$\mathrm{VED} = \frac{p}{vhd}, \tag{1}$$

where VED is the volumetric energy density of the powder bed (J/mm^3), P is the laser power (W), v is the laser scanning speed (mm/s), h is the hatch distance (mm), and d is the powder bed layer thickness (mm) [22, 23]. The measurement of porosity for the additively manufactured parts is essential in this technique. According to equation (2), the porosity can be measured by the Archimedes method. The manufactured body is firstly weighed at dry condition and then it is weighed while being suspended in water, and finally, the body is weighed at saturated condition after leaving it for 24 hours in the water [37].

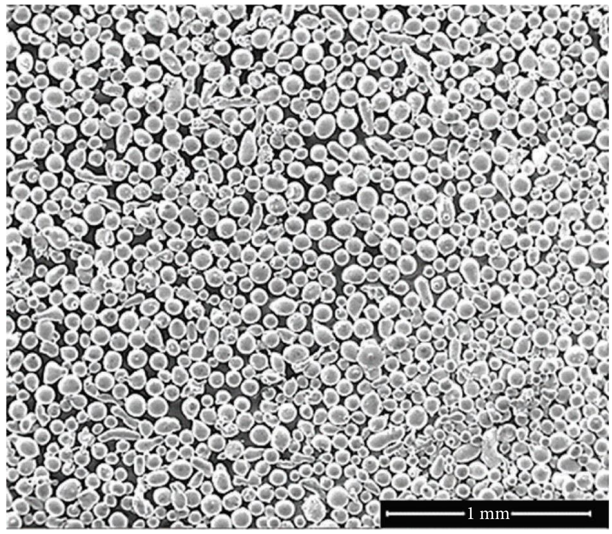

Figure 1: SEM for powder SS316L.

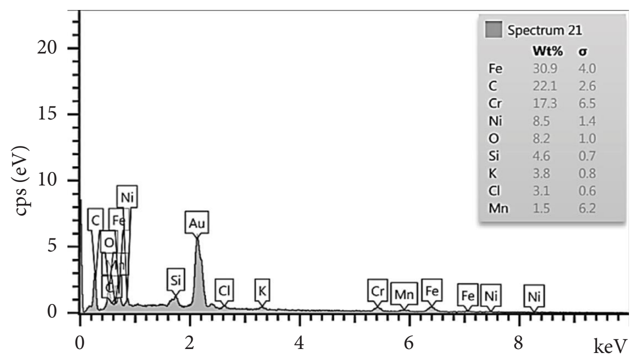

Figure 2: EDS of sample product by SLM.

Table 1: Chemical composition of stainless steel 316L (Wt. %).

Fe	C	Cr	Ni	Mn	Mo	P	Si
Bal.	0.03	17	12	2	2.5	0.05	1

$$\text{Porosity}\,\% = \frac{\text{weight of the saturated specimen} - \text{weight of the dry spcimen}}{\text{weight of the saturated specimen} - \text{weight of the soaked immersed specimen}}. \tag{2}$$

3. Results and Discussion

Following layer deposition, it is challenging to prevent process-induced flaws such as pores generated by the SLM process, non-optimal process parameters, powder contamination, and local voids. FESEM images of SiC-reinforced SS 316L samples were observed during the SLM preparation using a FESEM machine (Carl Zeiss, Germany) as shown in Figure 4(a).

The samples' images in Figure 4 reveal complete fusion at different magnifications. When ceramic particles are fused, an oxide layer forms on the surface of the particles, as shown in Figure 2. The SiC particles dissolve in the 316L matrix during manufacturing, leading to an increase in the proportion of reinforcement and a change in the matrix's composition. Oxides are formed (Fe_2O_3, Cr_2O_3, and Fe_3O_2) when silicon combines with Fe_3Si, as can be seen in Figure 5. Good wettability between SiC and SS 316L appears as there is no gap between the reinforcement interface and matrix, providing a solid metallic bond of Sic mixed with stainless steel. There were no small cracks when enlarging the image, despite the high heat which results in heat stress in the material due to the best parameters chosen, as shown in Figures 4(b)–4(d). The relation between the hardness values and the samples produced according to the results obtained for the hardness of the surface was between 277 HV and 296 HV as shown in Figure 6. It was found that the differences in hardness could be attributed to the scanning speed. At each scanning speed, the changes in the hardness value correspond to a certain scanning speed; by increasing

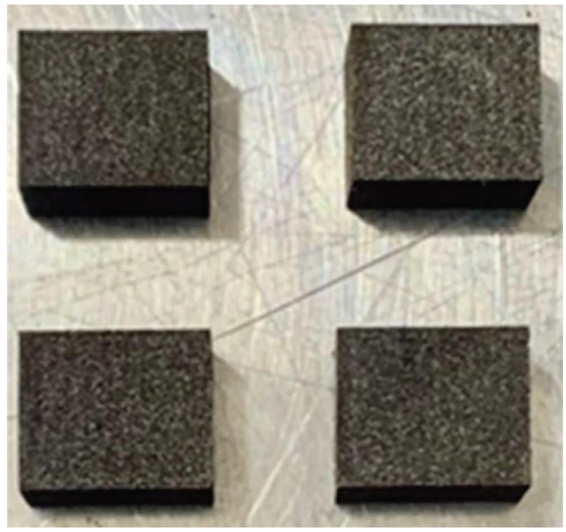

Figure 3: Dimensions of SLM as-manufacturing specimens ($10 \times 10 \times 10\,mm^3$).

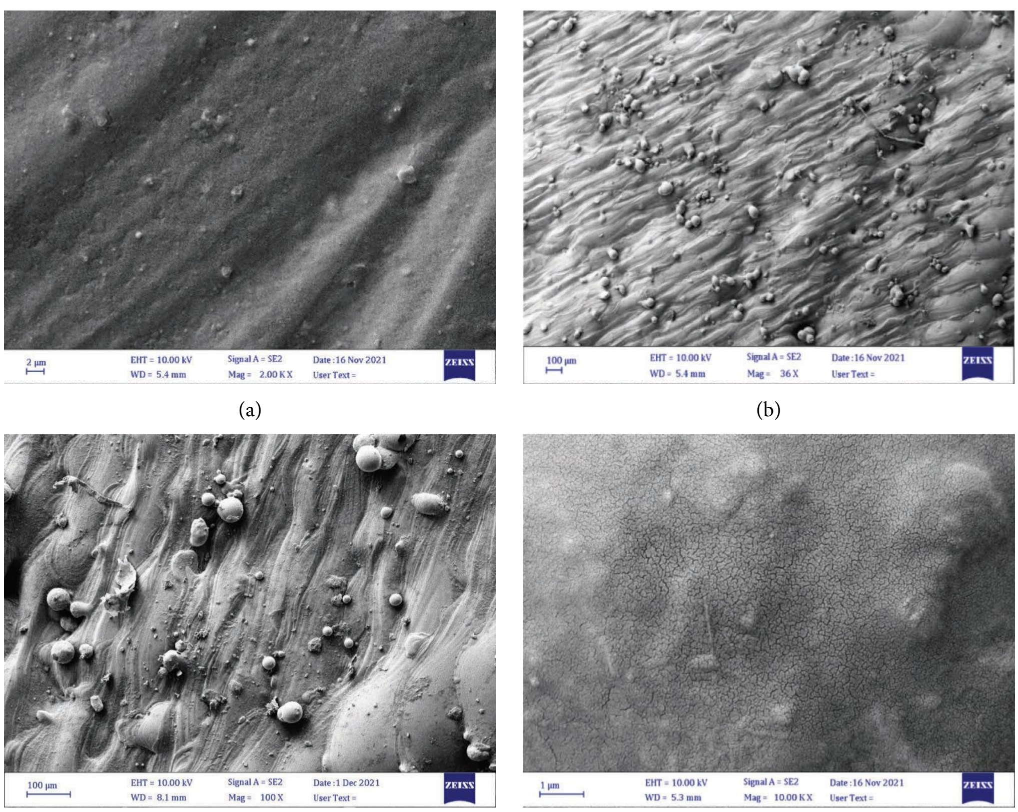

(a) (b)

(c) (d)

Figure 4: (a) FESEM image of the sample. (b) FESEM image of sample product by SLM with magnification of 36X. (c) FESEM image of sample product by SLM with magnification of 100X. (d) FESEM image of sample product by SLM with magnification of 10.00 kX.

the mass density of the samples, the hardness value also increases. The rational reason is that the developed defects can weaken the material strength, and the indenter can penetrate the Vickers hardness tester more effortlessly.

The maximal hardness achieved was 296 HV for S3 sample, as shown in Table 2, which has the highest density of 99.6% among the manufactured samples (Figure 7). The effect of scanning speed seems to be very important for the hardness and relative density alike, as the hardness is low at low speeds and high laser power. The residual heat in the material can cause undesirable consequences like agglomeration, keyhole and with pelleting phenomenon due to the high cooling rate and high laser power. This causes a change in the mechanical properties of the material.

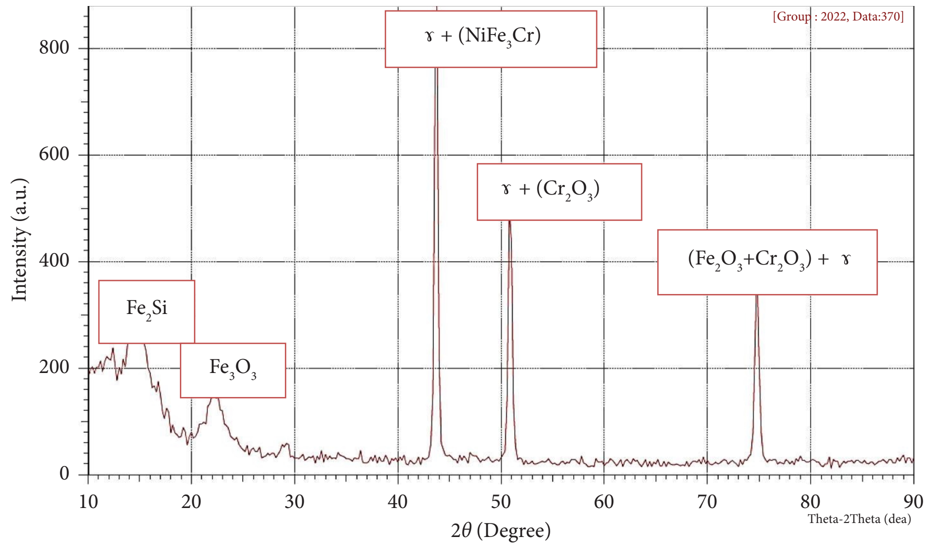

Figure 5: XRD patterns of stainless steel 316L with silicon carbide composite.

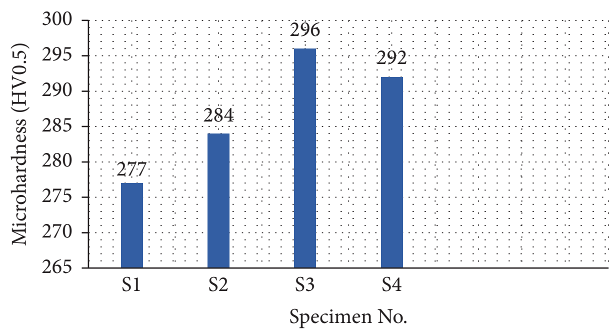

Figure 6: Microhardness (HV) for samples produced by SLM.

Table 2: The sample produced with constant layer thickness of 30 μm, hatch distance of 70 μm, and laser power of 200 W.

No. of sample	Scanning speed (mm/s)	VED (J/mm^3)	Microhardness (HV)
S1	500	190	277
S2	600	158	284
S3	700	136	296
S4	800	119	292

At high velocity, there will be incomplete melting of the material, and therefore the hardness will also be lower due to the voids that occur. Therefore, choosing the appropriate velocity with other parameters is very important to obtain accurate and suitable hardness for the product without these defects. The apparent increase in the rate of hardness means that the particles knit more strongly. The volumetric energy density was calculated from the parameters of the samples. After examining the porosity of the models and microhardness, the best VED chosen was 136 J/mm^3, as shown in Figures 8 and 9.

According to Figure 7, the relative density increases as the speed increases to a specific limit until the relative density of the body reaches its highest value, indicating the complete melting for the body with the stability of the laser energy density, which leads to filling the spaces between the molecules. Since the SLM technique is characterized as a procedure that has a high cooling rate, at high velocities, the fusion is incomplete; therefore, there will be gaps in the melting basin and the relative density will decrease.

The tensile test quantified the samples' tensile strength (Figure 10(a)). The tensile samples were prepared and tested at a junction velocity of 1 mm/min according to ASTM-E8. Forthe samples with 1% SiC, the rise in the load was found to reach about 60 kN (570MPa) to break the sample with only 8.1 distortion; whereas for 316L samples without SiC, it was 565 MPa and with 8.95 mm distortion (Figure 10(c)). Figure 11 depicts the fracture that occurred during the tensile test. For compression tests, in contrast, the samples were prepared and tested at transverse velocities of 1 mm/min according to ASTM- E9, as shown in Figure 12. For all samples, the load was fixed at 120 kN (1569 MPa), and the deformation in the model was calculated at this reading as in Figure 13. The distortion rate of the sample was less than that

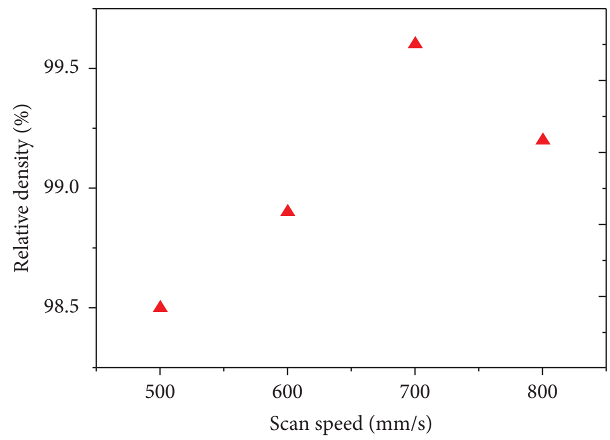

Figure 7: Relation between the relative density and scanning speed.

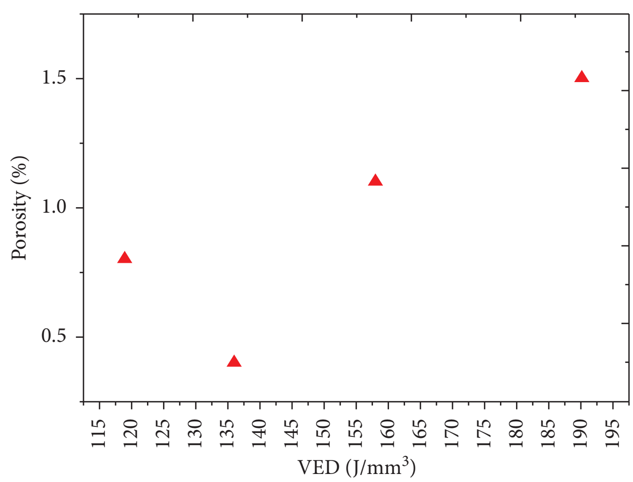

Figure 8: Porosity for product with volumetric energy density.

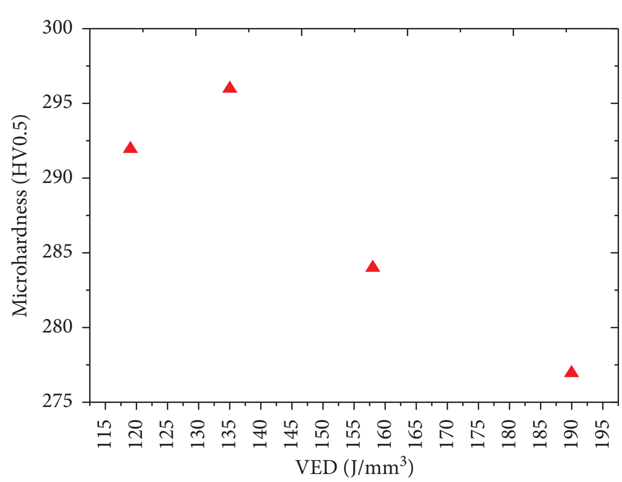

Figure 9: Microhardness for samples with volumetric energy density.

of stainless steel without silicon carbide. The maximum distortion of the sample was 9.2 mm, while the distortion of stainless steel was 9.85 mm; note that the same load has been applied to both samples—120 kN. The major contributing factor in increasing the strength of the samples is the presence of C rather than Si [38]. Increasing the SiC percentage in 316L MMC stainless steel leads to increased hardness but decreased wear resistance [39]. In the case of SLM 316L-SiC composites, migration of C (and Si) into the austenitic matrix could have occurred, introducing solid

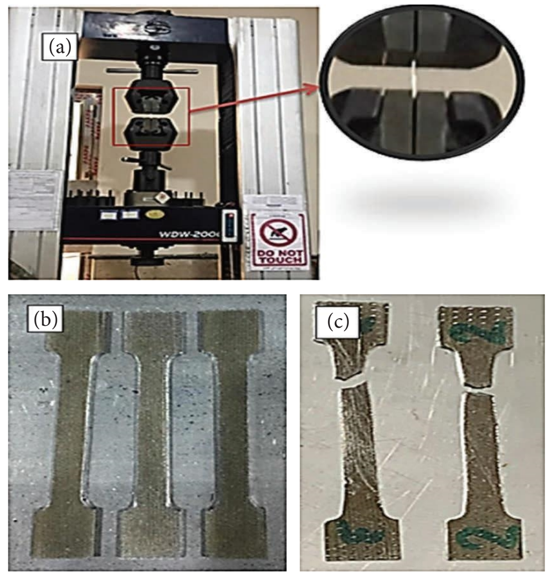

FIGURE 10: (a) The tensile testing machine for tensile strength. (b) Samples before testing. (c) Samples after testing.

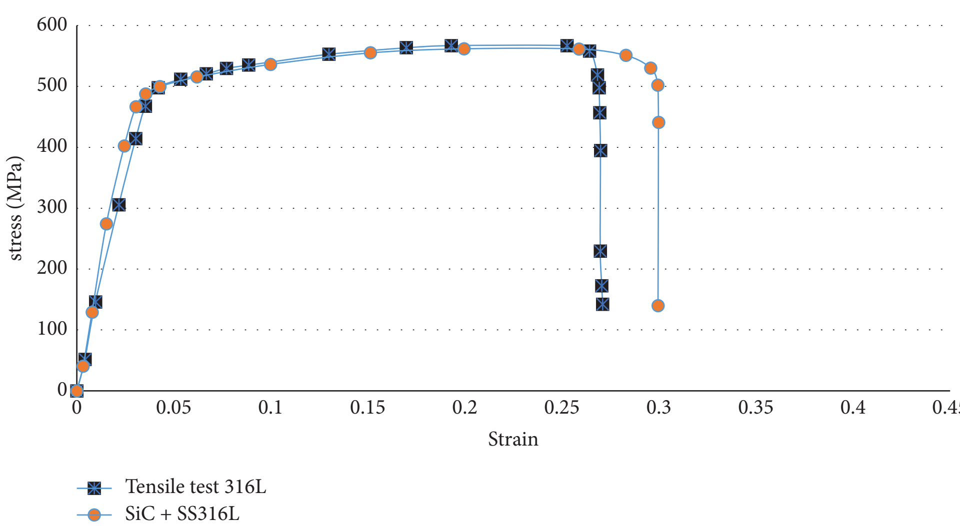

FIGURE 11: Tensile strength for breaking the samples 316L and 316L with 1% SiC.

Figure 12: (a) Compression testing. (b) Samples before testing. (c) Samples after testing.

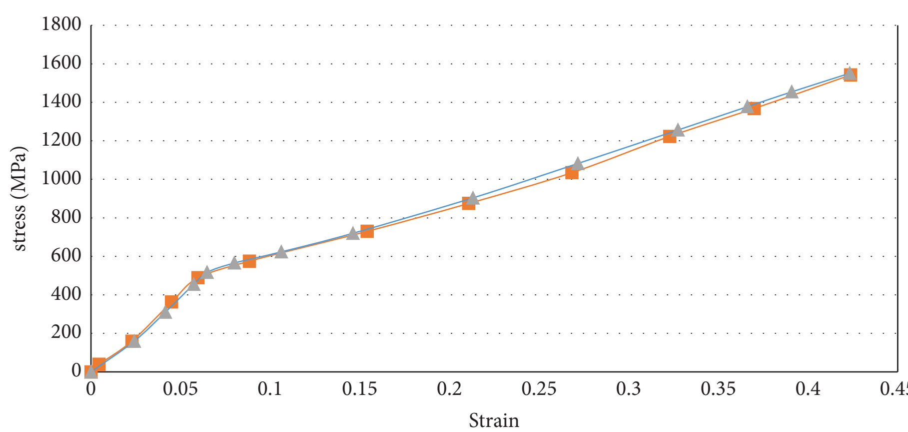

Figure 13: Compressive strength was 1560 MPa for the samples.

solution strengthening effects. Furthermore, particles at the austenite grain boundaries may be responsible for dislocation pinning, which contributes to the strength of the 316L-SiC composites [40].

4. Conclusions

Based on the selective laser melting method, the continuous wave fiber laser was used to successfully produce SS 316L MMCs that are enhanced with silicon carbide particles. The gaps at the interfaces between SiC and SS 316L phase were trivial, signifying the proper compatibility between reinforcement and matrix in the argon atmosphere. With different parameter settings, the fine SiC particles enhanced the microhardness of the 316L matrix. It was found that adding 1% of SiC improved the hardness and resulted in a high product density. A relative density of 99.6 was achieved in MMC samples. The scanning speed and the increased laser power were very crucial after setting other parameters such as hole spacing, layer thickness, and spot size in additive manufacturing utilizing a highly selective laser melting process. In addition, the tensile and compression strengths of the samples were higher than those in stainless steel without silicon carbide.

Data Availability

No data were used in this study.

Conflicts of Interest

The authors declare that they have no conflicts of interest.

References

[1] J. D. Kechagias, K. Ninikas, P. Stavropoulos, and K. Salonitis, "A generalised approach on kerf geometry prediction during CO_2 laser cut of PMMA thin plates using neural networks," *Lasers in Manufacturing and Materials Processing*, vol. 8, no. 3, pp. 372–393, 2021.

[2] J. D. Kechagias, N. A. Fountas, K. Ninikas, M. Petousis, N. Vidakis, and N. Vaxevanidis, "Surface characteristics investigation of 3D-printed PET-G plates during CO2 laser cutting," *Materials and Manufacturing Processes*, vol. 37, pp. 1–11, 2021.

[3] H. A. Jasim, A. G. Demir, B. Previtali, and Z. A. Taha, "Process development and monitoring in stripping of a highly transparent polymeric paint with ns-pulsed fiber laser," *Optics & Laser Technology*, vol. 93, pp. 60–66, 2017.

[4] Z. A. Taha, "Hole drilling of high density polyethylene using Nd: YAG pulsed laser," *Iraqi Journal of Laser*, vol. 18, pp. 41–46, 2019.

[5] F. A. Mutlak, M. Jaber, and H. Emad, "Effect of laser pulse energy on the characteristics of Au nanoparticles and applications in medicine," *Iraqi Journal of Science*, pp. 2364–2369, 2017.

[6] M. A. Obeidi, "Metal additive manufacturing by laser-powder bed fusion: Guidelines for process optimisation," *Results in Engineering*, Elsevier BV, vol. 15, Article ID 100473, 202273.

[7] N. Li, W. Liu, Y. Wang et al., "Laser additive manufacturing on metal matrix composites: a review," *Chinese Journal of Mechanical Engineering*, vol. 34, no. 1, pp. 38–16, 2021.

[8] J. P. Chen, L. Gu, and G. J. He, "A review on conventional and nonconventional machining of SiC particle-reinforced aluminium matrix composites," *Advances in Manufacturing*, vol. 8, no. 3, pp. 279–315, 2020.

[9] Szewczyk-Nykiel, "Microstructure and properties of sintered metal matrix composites reinforced with SiC particles," *Technical Transactions*, vol. 114, pp. 179–190, 2017.

[10] J. Platl, H. Leitner, C. Turk, A. G. Demir, B. Previtali, and R. Schnitzer, "Defects in a laser powder bed fused tool steel," *Advanced Engineering Materials*, vol. 23, no. 12, Article ID 2000833, 2021.

[11] K. V. Wong and A. Hernandez, "A review of additive manufacturing," *ISRN Mechanical Engineering*, Hindawi Limited, vol. 2012, Article ID 208760, 2012.

[12] W. Chen, L. Xu, Y. Zhang, Y. Han, L. Zhao, and H. Jing, "Additive manufacturing of high-performance 15-5PH stainless steel matrix composites," *Virtual and Physical Prototyping*, Informa UK Limited, vol. 17, no. 2, pp. 366–381, 2021.

[13] S. L. Sing, "Perspectives on additive manufacturing enabled beta- titanium alloys for biomedical applications," *International Journal of Bioprinting*, Whioce Publishing Pte Ltd, vol. 8, no. 1, Article ID 478, 2022.

[14] W. Yu, Z. Xiao, X. Zhang et al., "Processing and characterization of crack-free 7075 aluminum alloys with elemental Zr modification by laser powder bed fusion," *Materials Science in Additive Manufacturing*, vol. 1, no. 1, p. 4, 2022.

[15] C. Liang, Y. Hu, N. Liu et al., "Laser polishing of ti6al4v fabricated by selective laser melting," *Metals*, vol. 10, no. 2, 191 pages, 2020.

[16] H. K. Koh, J. G. S. Moo, S. L. Sing, and W. Y. Yeong, "Use of fumed silica nanostructured additives in selective laser melting and fabrication of steel matrix nanocomposites," *Materials*, vol. 15, no. 5, Article ID 1869, 1869.

[17] S. Bai, N. Perevoshchikova, Y. Sha, and X. Wu, "The effects of selective laser melting process parameters on relative density of the alsi10mg parts and suitable procedures of the archimedes method," *Applied Sciences*, vol. 9, no. 3, Article ID 583, 2019.

[18] B. Madejski, M. Malicki, S. Czarnewicz, and K. Gruber, "Microstructural and mechanical properties of selective laser melted Inconel 718 for different specimen sizes," *Fatigue of Aircraft Structures*, vol. 2020, no. 12, pp. 15–26, 2020.

[19] T. Xia, R. Wang, Z. Bi, G. Zhu, Q. Tan, and J. Zhang, "Effect of heat treatment on microstructure and mechanical properties of a selective laser melting processed Ni-based superalloy GTD222," *Materials*, vol. 14, no. 13, Article ID 3668, 2021.

[20] J. Kennedy, L. Flanagan, L. Dowling, G. J. Bennett, H. Rice, and D. Trimble, "The influence of additive manufacturing processes on the performance of a periodic acoustic metamaterial," *International Journal of Polymer Science*, vol. 2019, 2019.

[21] L. Alifui-Segbaya, W. Heine, H. Hall, M. Öchsner, and A. Ochsner, "Additive manufacturing of cobalt-based dental alloys: analysis of microstructure and physicomechanical properties," *Advances in Materials Science and Engineering*, vol. 2018, pp. 1–12, 2018.

[22] Y. Li, M. Založnik, J. Zollinger, L. Dembinski, and A. Mathieu, "Effects of the powder, laser parameters and surface conditions on the molten pool formation in the selective laser melting of In718," *Journal of Materials Processing Technology*, vol. 289, Article ID 116930, 2021.

[23] W. Yu, Xiao, Zhang et al., "Processing and characterization of crack-free 7075 aluminum alloys with elemental Zr modification by laser powder bed fusion," *Materials Science in Additive Manufacturing*, Whioce Publishing Pte Ltd, vol. 1, no. 1, p. 4, 2022.

[24] G. Pyka, Burakowski, Kerckhofs, Van Bael, J. Wevers, and M. Wevers, "Surface modification of Ti6Al4V open porous structures produced by additive manufacturing," *Advanced Engineering Materials*, vol. 14, no. 6, pp. 363–370, 2012.

[25] P. Konda Gokuldoss, "Design of next-generation alloys for additive manufacturing," *Material Design & Processing Communications*, vol. 1, no. 4, 2019.

[26] P. Yang, X. Guo, D. He, Z. Tan, W. Shao, and H. Fu, "Selective laser melting of high relative density and high strength parts made of minor surface oxidation treated pure copper powder," *Metals*, vol. 11, no. 12, Article ID 1883, 2021.

[27] M. Mokhtari, P. Pommier, Y. Balcaen, and J. Alexis, "Laser welding of AISI 316l stainless steel produced by additive manufacturing or by conventional processes," *Journal of Manufacturing and Materials Processing*, vol. 5, no. 4, Article ID 136, 2021.

[28] B. Schoinochoritis, D. Chantzis, and K. Salonitis, "Simulation of metallic powder bed additive manufacturing processes with the finite element method: a critical review," *Proceedings of the Institution of Mechanical Engineers - Part B: Journal of Engineering Manufacture*, SAGE Publications, vol. 231, no. 1, pp. 96–117, 2016.

[29] K. Chadha, Y. Tian, J. Spray, and C. Aranas, "Effect of annealing heat treatment on the microstructural evolution and mechanical properties of hot isostatic pressed 316L stainless steel fabricated by laser powder bed fusion," *Metals*, vol. 10, no. 6, Article ID 753, 2020.

[30] J. Liu, Y. Song, C. Chen et al., "Effect of scanning speed on the microstructure and mechanical behavior of 316L stainless steel fabricated by selective laser melting," *Materials & Design*, vol. 186, Article ID 108355, 2020.

[31] A. Ur RehmanUr Rehman, M. A. Saleem, T. Liu, K. Zhang, F. Pitir, and M. U. SalamciSalamci, "Influence of silicon carbide on direct powder bed selective laser process (sintering/melting) of alumina," *Materials*, vol. 15, no. 2, Article ID 637, 2022.

[32] Y. Zou, C. Tan, Z. Qiu, W. Ma, M. Kuang, and D. Zeng, "Additively manufactured SiC-reinforced stainless steel with excellent strength and wear resistance," *Additive Manufacturing*, vol. 41, Article ID 101971, 2021.

[33] A. Riquelme, C. Sánchez de Rojas Candela, P. Rodrigo, and J. Rams, "Influence of process parameters in additive manufacturing of highly reinforced 316L/SiCp composites," *Journal of Materials Processing Technology*, vol. 299, Article ID 117325, 2022.

[34] P. Wang, J. Eckert, K. G. Prashanth et al., "A review of particulate-reinforced aluminum matrix composites fabricated by selective laser melting," *Transactions of Nonferrous Metals Society of China*, vol. 30, no. 8, pp. 2001–2034, 2020.

[35] S. Zhao, X. Shen, J. Yang, W. Teng, and Y. Wang, "Densification behavior and mechanical properties of nanocrystalline tic reinforced 316l stainless steel composite parts fabricated by selective laser melting," *Optics & Laser Technology*, vol. 103, pp. 239–250, 2018.

[36] A. Mandal, J. K. Tiwari, B. AlMangour et al., "Tribological behavior of graphene-reinforced 316l stainless-steel composite prepared via selective laser melting," *Tribology International*, vol. 151, Article ID 106525, 2020.

[37] S. Misra, M. Hussain, A. Gupta, V. Kumar, S. Kumar, and A. K. Das, "Fabrication and characteristic evaluation of direct metal laser sintered SiC particulate reinforced Ti6Al4V metal matrix composites," *Journal of Laser Applications*, Laser Institute of America, vol. 31, no. 1, Article ID 012005, 2019.

[38] C. Wu, S. Zhang, C. Zhang, J. Zhang, Y. Liu, and J. Chen, "Effects of SiC content on phase evolution and corrosion behavior of SiC-reinforced 316L stainless steel matrix composites by laser melting deposition," *Optics & Laser Technology*, vol. 115, pp. 134–139, 2019.

[39] Y. T. Ang, S. L. Sing, and J. C. W. Lim, "Process study for directed energy deposition of 316L stainless steel with TiB2 metal matrix composites," *Materials Science in Additive Manufacturing*, vol. 1, no. 2, pp. 13–2, 2022.

[40] A. Mussatto, Groarke, Vijayaraghavan et al., "Laser-powder bed fusion of silicon carbide reinforced 316L stainless steel using a sinusoidal laser scanning strategy," *Journal of Materials Research and Technology*, Elsevier BV, vol. 18, pp. 2672–2698, 2022.